

Electronic Supplementary Information

Preparation of Au nanoparticles in a non-polar medium: obtaining high-efficiency nanofluid for Concentrating Solar Power. An experimental and theoretical perspective

Roberto Gómez-Villarejo,¹ Javier Navas,^{*,1} Elisa I. Martín,² Antonio Sánchez-
Coronilla,^{*,3} Teresa Aguilar,¹ Juan Jesús Gallardo,¹ Desiré De los Santos,¹ Rodrigo
Alcántara,¹ Concha Fernández-Lorenzo,¹ Joaquín Martín-Calleja¹

¹ Departamento de Química Física, Facultad de Ciencias, Universidad de Cádiz, E-11510 Puerto Real (Cádiz), Spain;

² Departamento de Ingeniería Química, Facultad de Química, Universidad de Sevilla, E-41012 Sevilla, Spain;

³ Departamento de Química Física, Facultad de Farmacia, Universidad de Sevilla, E-41012 Sevilla, Spain.

Corresponding Authors:

*Javier Navas (javier.navas@uca.es); Antonio Sánchez-Coronilla (antsancor@us.es).

Characterization of nanoparticles and nanofluids

In order to corroborate the synthesis of gold nanoparticles in the base fluid, several techniques were required. The chemical state bonding and the oxidation states of the solid extracted from the nanofluids were studied by x-ray photoelectron spectroscopy (XPS). The XPS spectra were recorded using a Kratos Axis UltraDLD spectrometer, with monochromatic Al K α radiation (1486.6 eV) and 20 eV pass energy. The binding energy scale was given with an accuracy of 0.1 eV. Electrostatic charging effects could be stabilized with the help of the specific device developed by Kratos. Transmission Electron Microscopy (TEM) was used to observe the size and shape of the nanoparticles. TEM analysis was performed using a JEM-2100F microscope supplied by Jeol©. In turn, x-ray diffraction (XRD) was used to determine the crystalline phases in the solid extracted from nanofluids. The patterns were recorded using a D8 Advance diffractometer supplied by Bruker® with Cu-K α radiation. The scan conditions were from 10 to 75° in 2 θ with a resolution of 0.02°, 40 kV and 40 mA.

Stability is one of the key concepts in nanofluids because their thermal properties depend heavily on whether they are stable or unstable. UV-vis spectroscopy (UV-vis) can provide a measurable characterization of stability by evaluating the absorbance of a suspension.¹ To this end, UV-vis spectra were recorded using a halogen lamp DH-2000-Bal supplied by OceanOptics© and a monochromator USB-2000+ supplied by OceanOptics© operating in the range of wavelength of 400-880 nm, using a glass cuvette at room temperature. Also, ζ potential measurements were performed using Zetasizer Nano ZS supplied by Malvern Instruments Ltd. This system uses the principle of Electrophoresis Light Scattering (ELS), in which charged particles suspended in a fluid are attracted towards the oppositely charged electrode when an electric field is applied. The ζ potential measurements were performed applying a potential of 120 V at

313 K, and the results were analysed using the Huckel model, typical for low dielectric constant fluids. Particle size and size distribution was also measured by Zetasizer Nano ZS, using the principle of Dynamic Light Scattering (DLS) as a simple method for analysing suspension stability and particle size measurements in solution.^{2,3}

Density, viscosity, isobaric specific heat and thermal conductivity were determined to characterize the nanofluids performance, taking into consideration their application as a new class of heat transfer fluid in solar collectors in CSP. Density was estimated using a pycnometer and a thermal bath supplied by Select© to control the temperature of the measurements. The density values of each nanofluid were determined five times to obtain the most accurate value. Dynamic viscosity was measured using a SV-10 viscometer supplied by Malvern Instruments Ltd. A water-circulating bath supplied by VWR© with heating and cooling features was used to keep the nanofluids at room temperature during the experiment. The measurements were performed five times to calculate the average values. The isobaric specific heat measurements were performed using a Temperature Modulated Differential Scanning Calorimeter (TMDSC), supplied by TA Instruments©, model Q-20. To perform the measurements, a program was created which can be summarized as: the temperature was equilibrated at 341 K to remove contaminants and kept isothermal for 10 min; then the samples were equilibrated at 301 K and then ramped to 391 K at 1 K/min. A modulation was programmed around the studied temperatures with an amplitude of ± 1 K a period of 120 seconds. Finally, cooling was performed at 1 K/min. The isobaric specific heat of the base fluid was measured to test the method used with regard to the values reported by the supplier. Finally, the thermal conductivity of the nanofluids was measured at several temperatures using the laser flash technique (LFA 1600 equipment, supplied by Linseis Thermal Analysis©). This technique really measures thermal diffusivity, which

is the thermophysical property that defines the speed of heat propagation by conduction during changes of temperature. According to Standard ASTM E 1461-01 the relationship between both properties is given by the equation:

$$k(T) = D(T) \cdot C_p(T) \cdot \rho(T) \quad (1)$$

where k is the thermal conductivity, D the thermal diffusivity, C_p is the isobaric specific heat and ρ is the density. All the thermal measurements were performed in triplicate.

Results and discussion. XPS analysis

Figure S1 in the Electronic Supplementary Material (ESI) shows the general x-ray photoelectron spectra and the basic assignment of the peaks found. It shows the presence of N from the remains of TOAB and Mo from the sample holder used.

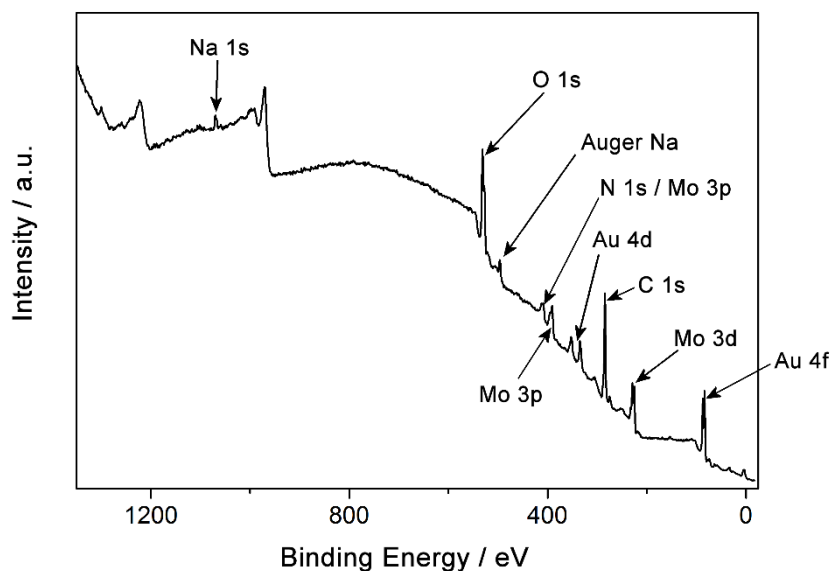


Figure S1. General XPS spectrum for the Au nanoparticles synthesized.

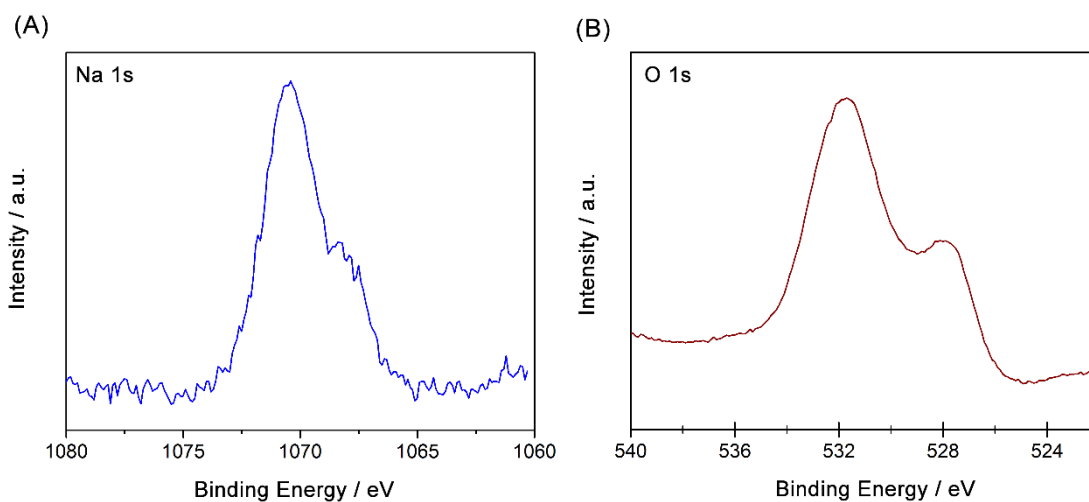


Figure S2. (A) Na 1s and (B) O 1s signals obtained from the XPS measurements performed for the Au nanoparticles synthesized.

Results and discussion. Nanofluid stability

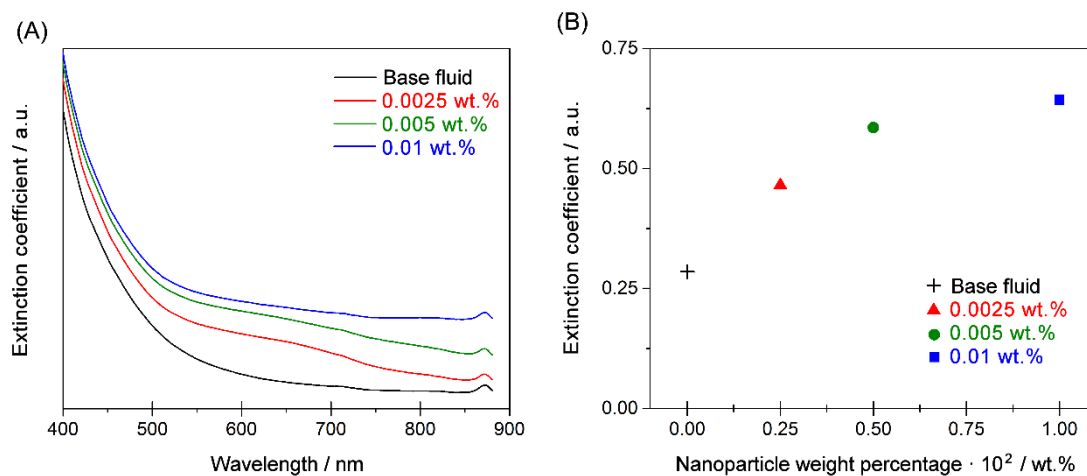


Figure S3. (A) UV-vis spectra obtained for the nanofluids at zero time. (B) Absorbance values at $\lambda = 520$ nm for the nanofluids prepared according to nanoparticle weight percentage.

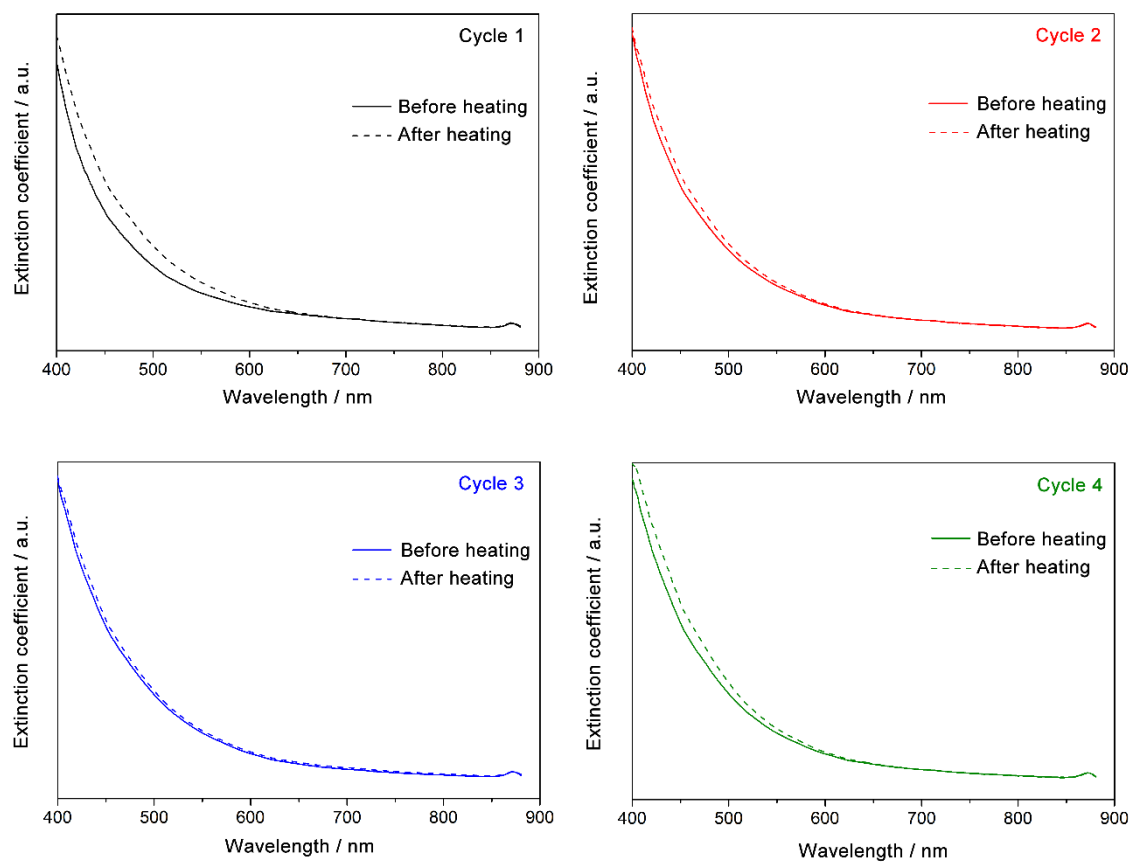


Figure S4. UV-vis spectra obtained for the nanofluent with a nominal concentration of 0.005 wt.% treated to heating/cooling cycles.

Results and discussion. Nanofluids performance

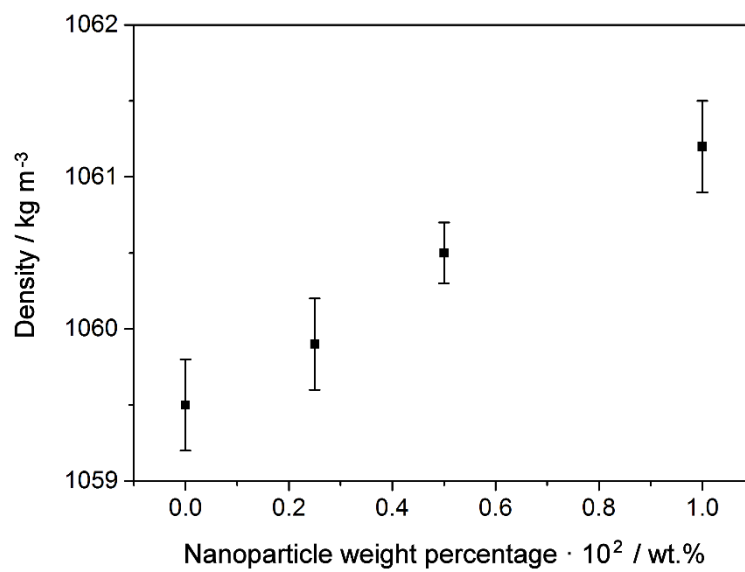


Figure S5. Density values of the nanofluids prepared versus nanoparticle weight percentage.

Hamilton-Crosser model and modified Hamilton-Crosser model

The classic model for thermal conduction is that of Hamilton-Crosser (H-C),⁴ defined according to

$$\frac{k_{nf}}{k_{bf}} = \frac{k_p + (n-1)k_{bf} - (n-1)\phi(k_{bf} - k_p)}{k_p + (n-1)k_{bf} + \phi(k_{bf} - k_p)} \quad (2)$$

where k_p is the thermal conductivity of the nanoparticles, $n=3/\Psi$ being $\Psi=1$ for spherical nanoparticles, and the remaining variables and sub-indexes have already been defined. In turn, the conventional H-C model can be modified to predict the effective thermal conductivity of nanofluids for nanoparticles in the form of aggregates as⁵

$$\frac{k_{nf}}{k_{bf}} = \frac{k_a + (n-1)k_{bf} - (n-1)\phi_{eff}(k_{bf} - k_a)}{k_a + (n-1)k_{bf} + \phi_{eff}(k_{bf} - k_a)} \quad (3)$$

where k_a is the thermal conductivity of the aggregates, which is estimated using the Bruggeman model for spherical nanoparticles⁶ according to

$$\frac{k_a}{k_{bf}} = \frac{1}{4} \left\{ (3\phi_{in} - 1) \frac{k_p}{k_{bf}} + [3(1 - \phi_{in}) - 1] \right. \\ \left. + \left[\left((3\phi_{in} - 1) \frac{k_p}{k_{bf}} + [3(1 - \phi_{in}) - 1] \right)^2 + 8 \frac{k_p}{k_0} \right]^{1/2} \right\} \quad (4)$$

where ϕ_{in} is the solid volume fraction of aggregates given by $\phi_{in} = \phi(a_a/a)^{D-3}$ ⁷, and a_a and a have been defined previously. In this model, the effective volume fraction and the thermal conductivity of aggregates are included.

Parameters of Hamilton-Crosser conduction model with a Brownian motion driven convective model

Koo and Kleinstreuer introduced a model to estimate the thermal conductivity of nanofluids composed of spherical particles. It combines the Hamilton-Crosser conduction model with a Brownian motion driven convective model.^{8,9}

$$k_{nf} = \frac{k_p + 2k_{bf} - 2\phi(k_{bf} - k_p)}{k_p + 2k_{bf} + \phi(k_{bf} - k_p)}k_{bf} + 5 \cdot 10^4 \beta \phi \rho_{bf} C_{P,bf} \sqrt{\frac{\kappa T}{\rho_p d_p}} f(T, \phi) \quad (5)$$

where $C_{P,bf}$ is the isobaric specific heat for the base fluid, ρ_p and d_p is the density and diameter of the nanoparticle, and κ is the Boltzmann constant. The factors β y $f(T, \phi)$ can be adjusted to the experimental data. β is a function of ϕ and depends on the type of nanoparticles. $f(T, \phi)$ is a function of T y ϕ . The first term represents static conductivity, while the second is the dynamic part that predicts the increase in conductivity due to Brownian motion. In turn, due to the presence of aggregates in the nanofluids prepared in this study, the modified Hamilton-Crosser model was included in the Koo and Kleinstreuer one to model the conduction process. This took into account the effective volume fraction, the thermal conductivity of aggregates and the diameter of the aggregates obtained using the DLS technique for the nanofluid studied, as has been shown previously. Thus, the mathematical expression for the model used is

$$\frac{k_{nf}}{k_{bf}} = \frac{k_a + 2k_{bf} - 2\phi_{eff}(k_{bf} - k_a)}{k_a + 2k_{bf} + \phi_{eff}(k_{bf} - k_a)} + \frac{1}{k_{bf}} 5 \cdot 10^4 \beta \phi_{eff} \rho_{bf} C_{P,bf} \sqrt{\frac{\kappa T}{\rho_p d_a}} f(T, \phi) \quad (6)$$

The results obtained are shown in Figure 7C in the main article. The β and $f(T, \phi)$ values for the results obtained are shown in Table S1. In turn, the values obtained for β and $f(T, \phi)$ are close to those reported previously.¹⁰ It is also seen that β does not change and $f(T, \phi)$ increases with the temperature, as the model predicts. β depends on the kind of

nanoparticles, so it is coherent that there is practically no change in this case because the same type of nanoparticles were used in all the nanofluids. In turn, $f(T, \phi)$ increases with temperature, as expected,¹⁰ again showing that the prediction of the values by this model, taking into account the effective volume fraction, is in agreement with the results obtained experimentally.

Table S1. β and $f(T, \phi)$ values for the plots in Figure 7C in the main article.

Temperature / K	β	$f(T, \phi)$
297.15	5.7	0.009
318.45	5.7	0.015
341.15	5.7	0.018
363.15	5.8	0.020

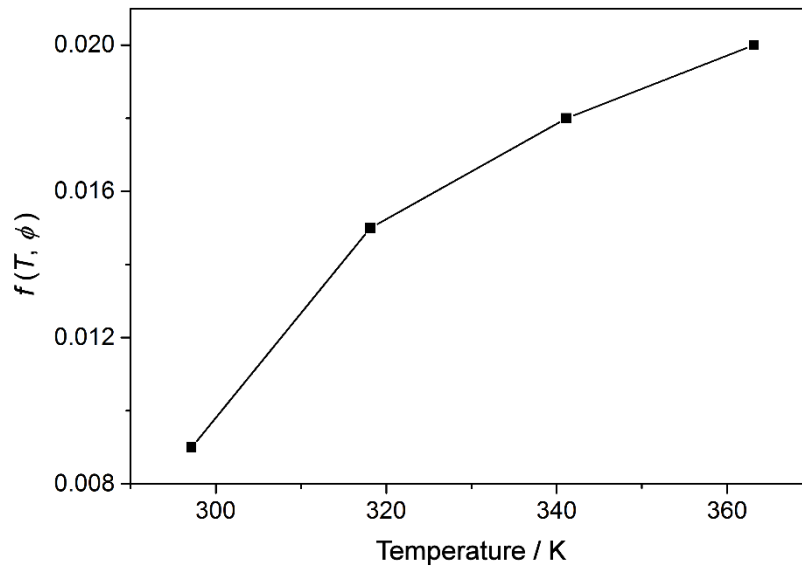


Figure S6. $f(T, \phi)$ values obtained for the simulated values of thermal conductivity from equation (2).

Figure of Merit based on Mouromtseff number

Under turbulent conditions flow, a Figure of Merit based on the Mouromtseff number (Mo) can be used. The Mouromtseff number is defined as

$$Mo = \frac{\rho^{0.8} \cdot k^{0.67} \cdot C_P^{0.33}}{\mu^{0.47}} \quad (7)$$

where ρ is the density, k the thermal conductivity, C_P the isobaric specific heat, and μ the dynamic viscosity. A high Mo value indicates that the fluid has a high energy transfer capacity, so the highest possible value is desirable for the Mo_{nf}/Mo_{bf} ratio. Thus, values higher than 1 imply that the nanofluid has a greater capacity than the base fluid. Figure S6 shows the values obtained for the Mo_{nf}/Mo_{bf} ratio for all the nanofluids at the measured temperatures. Compared with the base fluid, the nanofluid presents an increase in efficiency, just over 40% for the fluid with the highest effective volume fraction of nanoparticles.

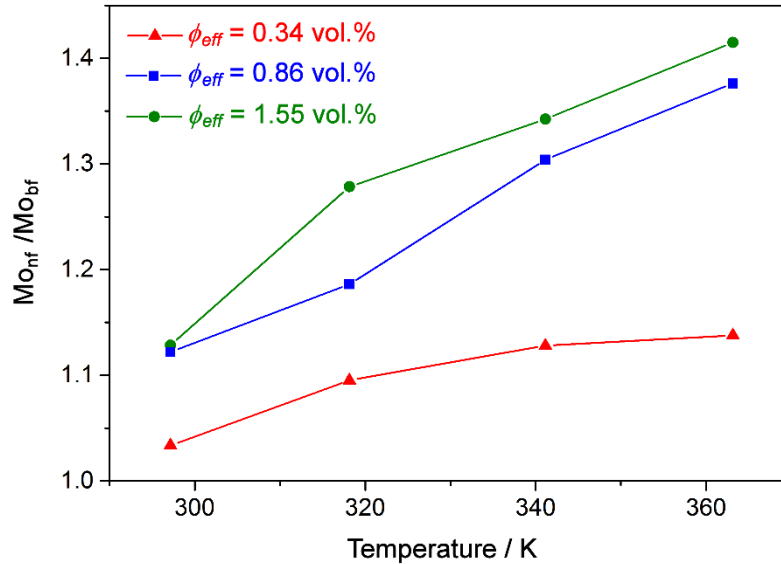


Figure S7. Mo_{nf}/Mo_{bf} ratio values for the nanofluids prepared.

Calculation of translational diffusion coefficient

The translational diffusion coefficients of base fluid and Au-nanofluid were computed according to the Einstein ratio by computing the mean square displacement (MSD). This translational diffusion coefficient is the thermal diffusivity used typically in experimental studies, as is discussed above. Thus, the diffusion coefficients are obtained by the following equation:

$$D_i = \lim_{t \rightarrow \infty} \frac{\langle |\vec{r}_i(t) - \vec{r}_i(0)|^2 \rangle}{6t} \quad (8)$$

where $\langle |\vec{r}_i(t) - \vec{r}_i(0)|^2 \rangle$ is the mean square displacement (MSD).

Figure S7A shows the plot of the mean square displacement (MSD) versus time for the Au-nanofluid system with the surfactant at varying temperatures. In each case, after approximately 3-4 ps the mean square displacement varies in line with time. The diffusion coefficients for both the Au-nanofluid system with surfactant, and the base fluid, versus temperature are obtained according equation (8) from the slope of the linear relationship (Figure S7B).

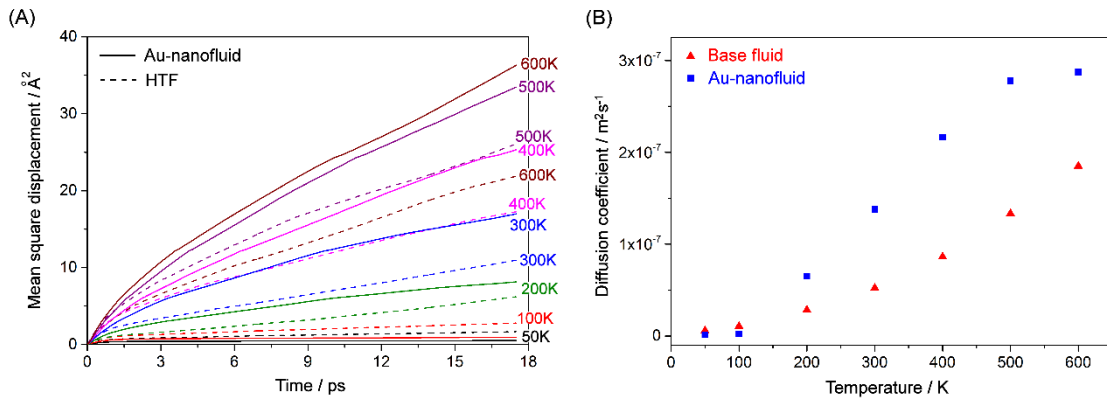


Figure S8. (A) Mean square displacement for Au-nanofluid and the base fluid at several temperatures. (B) The diffusion coefficient estimated from the mean square displacement.

References

1. W. S. Sarsam, A. Amiri, M. N. M. Zubir, H. Yarmand, S. N. Kazi and A. Badarudin, *Colloid Surface A*, 2016, **500**, 17-31.
2. S. A. Angayarkanni and J. Philip, *Adv Colloid Interfac*, 2015, **225**, 146-176.
3. R. C. Murdock, L. Braydich-Stolle, A. M. Schrand, J. J. Schlager and S. M. Hussain, *Toxicol Sci*, 2008, **101**, 239-253.
4. R. L. Hamilton and O. K. Crosser, *Ind Eng Chem Fund*, 1962, **1**, 187-&.
5. H. Y. Chen, S. Witharana, Y. Jin, Y. L. Ding and C. Kim, Sri Lanka, 2008.
6. D. A. G. Bruggeman, *Ann Phys-Berlin*, 1935, **24**, 636-664.
7. J. W. Goodwin and R. W. Hughes, *Rheology for Chemists : An Introduction*, The Royal Society of Chemistry, Cambridge, UK, 2nd Edition edn., 2008.
8. J. Koo and C. Kleinstreuer, *J Nanopart Res*, 2004, **6**, 577-588.
9. R. S. Vajjha and D. K. Das, *Int J Heat Mass Tran*, 2012, **55**, 4063-4078.
10. R. S. Vajjha and D. K. Das, *Int J Heat Mass Tran*, 2009, **52**, 4675-4682.